Influence of color operator on Husky Hussar data

Sina Esmaeili and Gary F. Margrave

ABSTRACT

The real seismic section, even after excellent data processing, is always very bandlimited, lacking both low and high frequencies. In this situation, recovering any of this bandwidth can be helpful. Especially, at the low frequencies, missing any of this information can effect remarkably the impedance estimation. Data that has been deconvolved will usually have a white spectrum whereas well logs show a roll off in spectral amplitude at the low frequencies that is called "color". Using a color operator can restore this spectral color.

In this study, the effect of three different color operators on Husky Hussar data has been investigated. The results also are compared with the Colored Inversion method which is a popular way to compute a bandlimited impedance inversion with spectral color. These results demonstrate that using the color operator can improve the impedance results significantly.

INTRODUCTION

Inversion of seismic data to Acoustic Impedance (AI) because of band-limited seismic data is always challenging. In case of broadband seismic data, the recursion formula (Oldenburg et. al., 1983) is working perfectly and can estimate the acoustic impedance with all frequencies. However, in the real world the recorded seismic data because of number of reasons such as bandlimited nature of source wavelet, noise contamination, attenuation, absorption and etc. the recorded data are always bandlimited. Thus, the calculated acoustic impedance from recursion formula in this case is very inaccurate, missing both low and high frequencies. Missing the high frequency is causing resolution reduction and the loss of the low frequencies which most greatly hampers interpretation of the derived acoustic impedance. Galbrith and Millington (1979) used the acoustic impedance measured at a nearby well. Lavergne and Willm (1977) and Lindseth (1979) both added low frequencies derived from velocity analysis. In 1996, Ferguson and Margrave created the BLIMP (BandLimited IMPedance) inversion algorithm which extracts the low frequency data from well log data and applies them to the bandlimited inverted impedance.

Beside these, the bandlimited acoustic impedance can be calculated from other methods than recursion formula. The Colored Inversion (CI) is a simple and fast technique to invert the band-limited seismic data to relative impedance (Lancaster and Whitcombe, 2000). This is done by generating a single operator to match the average seismic spectrum to the shape of the well log impedance spectrum. From their observation, the AI spectra can be written as power law such as

$$S_{AI} \propto f^{\alpha} \ , \tag{1}$$

where f is frequency and the α term is a negative constant number. The α can be found for a field by curve-fitting to AI logs then the amplitude spectrum of the inversion operator is determined as being that which maps the seismic spectrum to a curve of form f^{α}. Once the inversion operator derived it should be applied to the deconvolved trace to create the acoustic impedance. Note that the colored inversion operator creates the band limited acoustic impedance. For example, figure.1 shows the performance of this method in compare with the recursion formula method for impedance estimation of one of the Husky Hussar wells located in east of Calgary, Alberta. The 10Hz low cut-off frequency applied for well impedance.

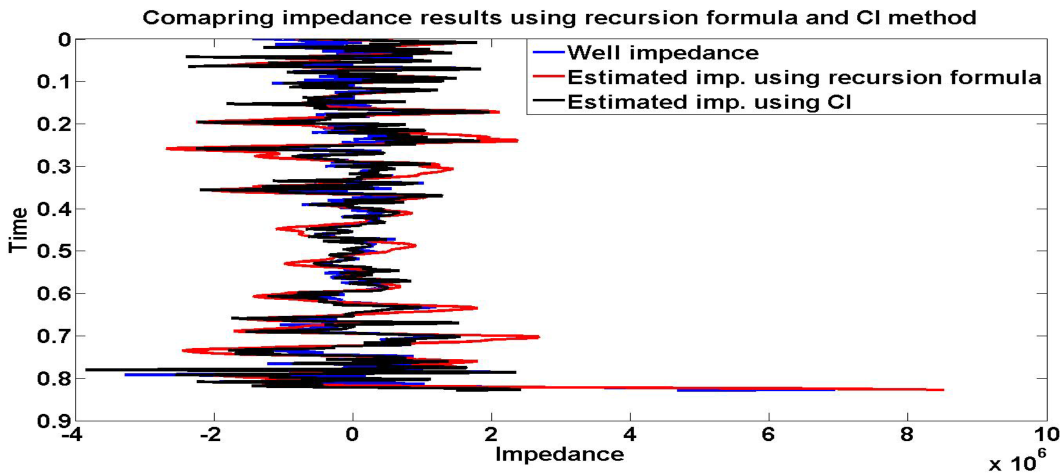

Fig. 1. Showing how the colored inversion can estimate the impedance's variation. 10Hz low cut-off frequency applied for well impedance and the colored inversion trace has been balanced with it.

The simple observation of colored inversion operator shows this operator is proportional to -90 degree phase rotation of seismic data. This can be seen from the comparison of amplitude spectra of -90 degree rotated seismic data and applied colored inversion operator to the seismic data (Figure 2). Also in the next figure (Figure 3) both data balanced with the 10Hz low-cut bandlimited well impedance.

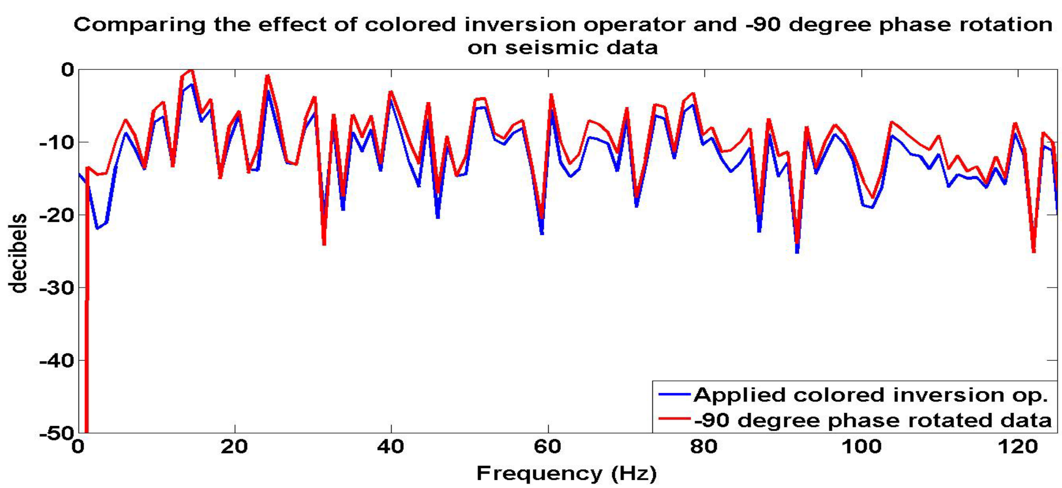

FIG. 2. The colored inversion can be approximated as -90 degree phase rotation of seismic data. Comparing the amplitude spectrum of -90 degree phase rotated seismic data and colored inversion trace can show this fact.

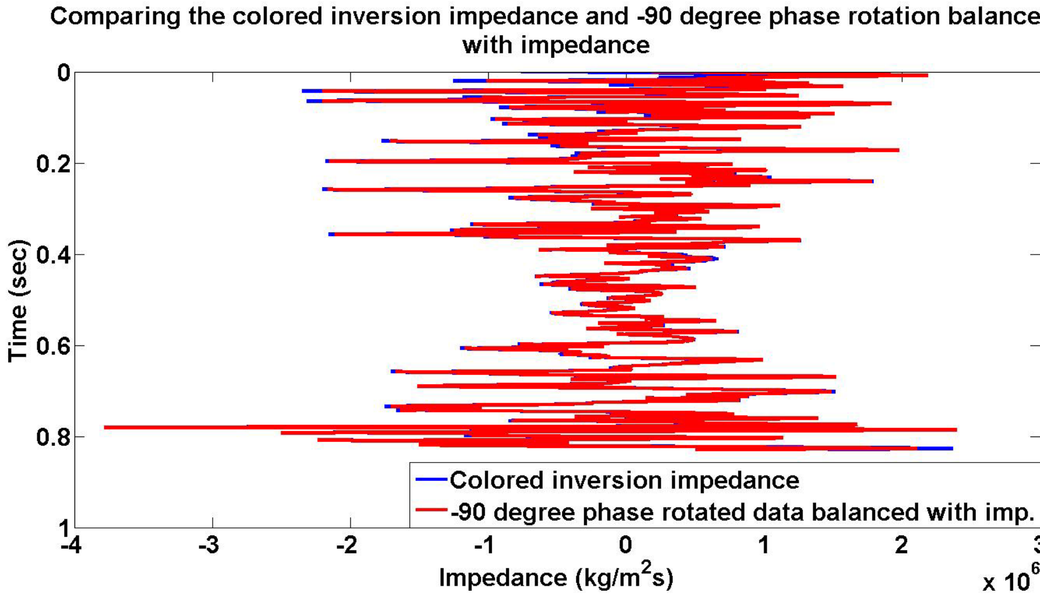

FIG. 3. Both colored inversion trace and -90 degree phase rotated seismic trace have been balanced with 13Hz low cut off well impedance.

The recursion formula (equation 2) suggests that to compute the acoustic impedance all we need to have the estimated reflectivity function. The reflectivity function can be obtained from deconvolving the seismic data.

$$I_n = I_1 \prod_{j}^{n} \left(e^{2R_j} \right) = I_1 e^{2\sum_{j=1}^{n} R_j} . \tag{2}$$

Esmaeili and Margrave (2014) showed the frequency domain deconvolution can be modeled with different algorithms. Three different algorithms based on three different smoother types were investigated to smooth the spectrum of seismic data and their results illustrated that for synthetic seismic data created from well log data the boxcar smoother can be the optimum choice in deconvolution algorithm. The synthetic data can be created via convolving the reflectivity function which computed from sonic and density log of the same well and an appropriate wavelet. This can be done with "seismo" which is in CREWES Matlab toolbox. In this study the minimum phase wavelet with 15Hz dominant frequency and 2 milliseconds sample rate has been chosen and the well log data is belonged to the Husky Hussar experiment located in east of Calgary, Alberta (Figure 4). Also, in figure 5 the result of amplitude spectrum of deconvolved data after applying frequency domain deconvolution with boxcar smoother with the length of 23Hz is shown. When the minimum phase deconvolution operator applying to the seismic data which has colored spectrum, because the algorithm is assuming the well reflectivity must has the white spectrum, the amplitude spectrum of deconvolved trace is following the white spectrum trace. This can be seen in the figure 5 where the spectrum of deconvolved trace before 60Hz instead of rolling off based on reflectivity's spectrum shape, its spectrum is becoming flat.

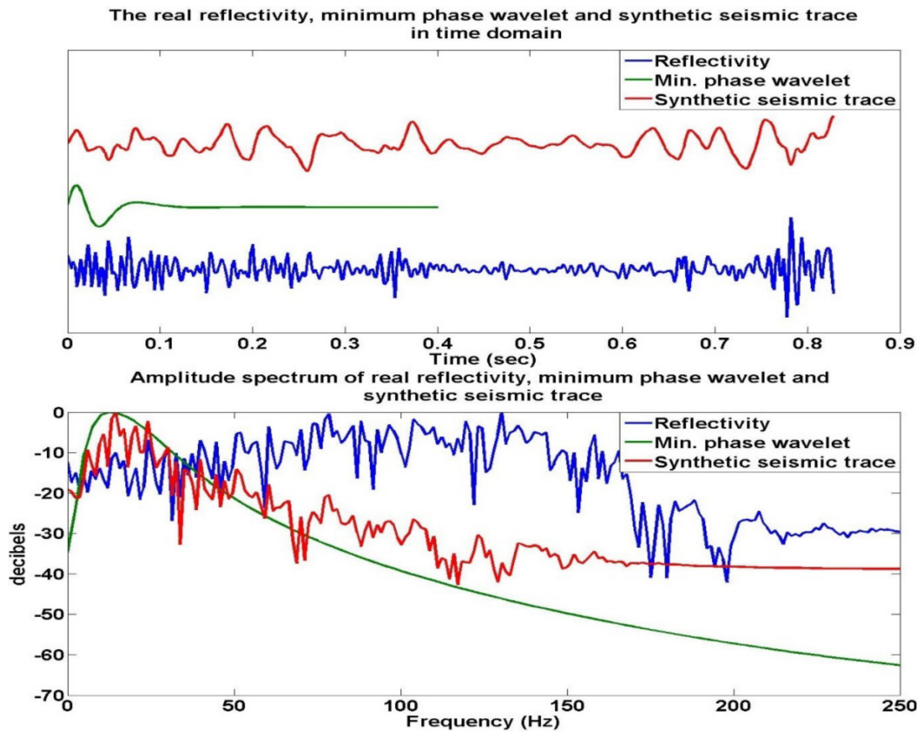

FIG. 4. The synthetic seismic trace created with “seismo” in Matlab CREWES toolbox. The synthetic seismic trace, minimum phase wavelet with 15Hz dominant frequency and Husky Hussar well reflectivity have been shown in both time (top) and frequency (bottom) domain.

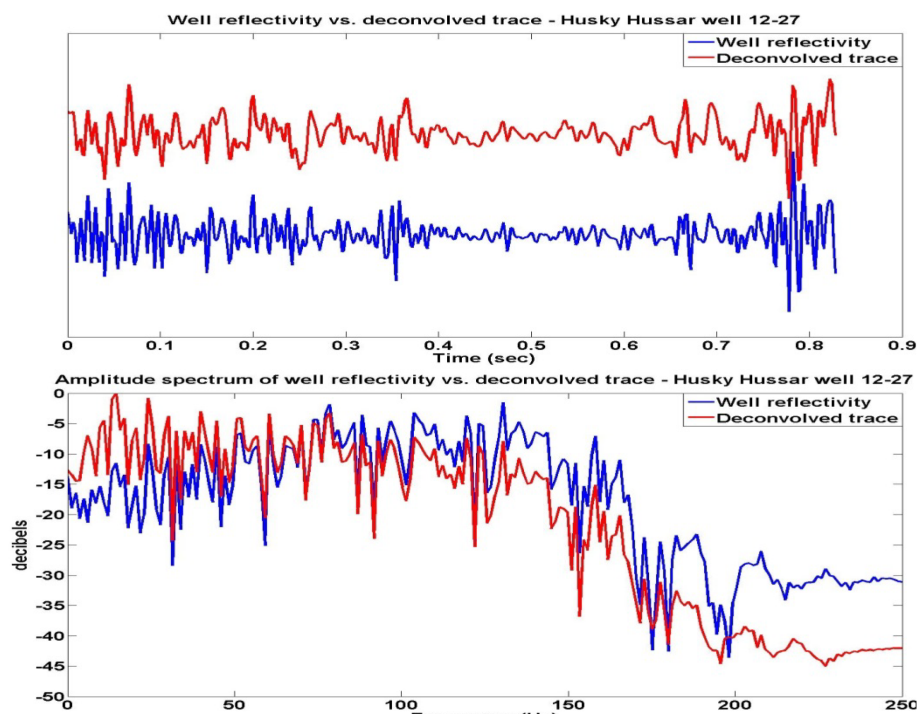

FIG. 5. The deconvolved seismic trace in time (time) and frequency (bottom) domain. The frequency domain deconvolution with boxcar smoother has been used.

To improve the acoustic impedance estimation, one possible idea is correcting this flatten area in frequency domain which can be done by designing the color operator. The objective of the color correction techniques is to create a model that represents the "colored" trend in the spectrum without reproducing the specific characteristics of reflectivity that must be preserved in the seismic; such as the reflections to be interpreted. For instance, one method which introduced by Hunt et. al. (1993) is deriving a color operator from the autocorrelation of real reflectivity. Once this operator was designed it can be applied to the deconvolved trace. The operator derivation can be done by multiplying the specific window to the reflectivity autocorrelation and that means in frequency domain it is equivalent to the smoothed power spectrum of reflectivity. Once the operator was applied to the deconvolved trace, the acoustic impedance can be calculated via recursion formula. Here, again for the same well log data from Husky Hussar (Well 12-27) the AutoCorrelation (AC) color operator has been derived via multiplying the Gaussian window into the autocorrelation of well reflectivity and then it has been transferred into the frequency domain. The well reflectivity's amplitude spectrum and its AC color operator are shown in decibels in Figure 4.

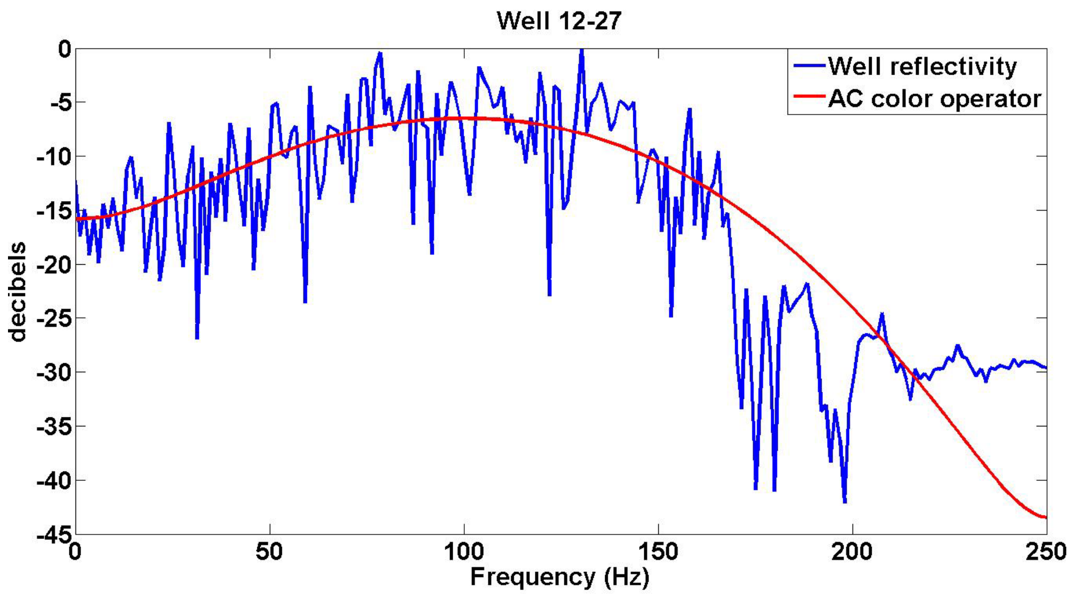

FIG. 6. The amplitude spectrum of Husky Hussar well 12-27 reflectivity and its AutoCorrelation (AC) color operator.

This color operator can be applied to the deconvolved seismic data which is shown in figure 5 and the result can be seen in figure 7 which shows in time and frequency domain. This figure shows how the AC color operator can correct the white spectrum part of deconvolved data. More impedance results will be shown at the next section.

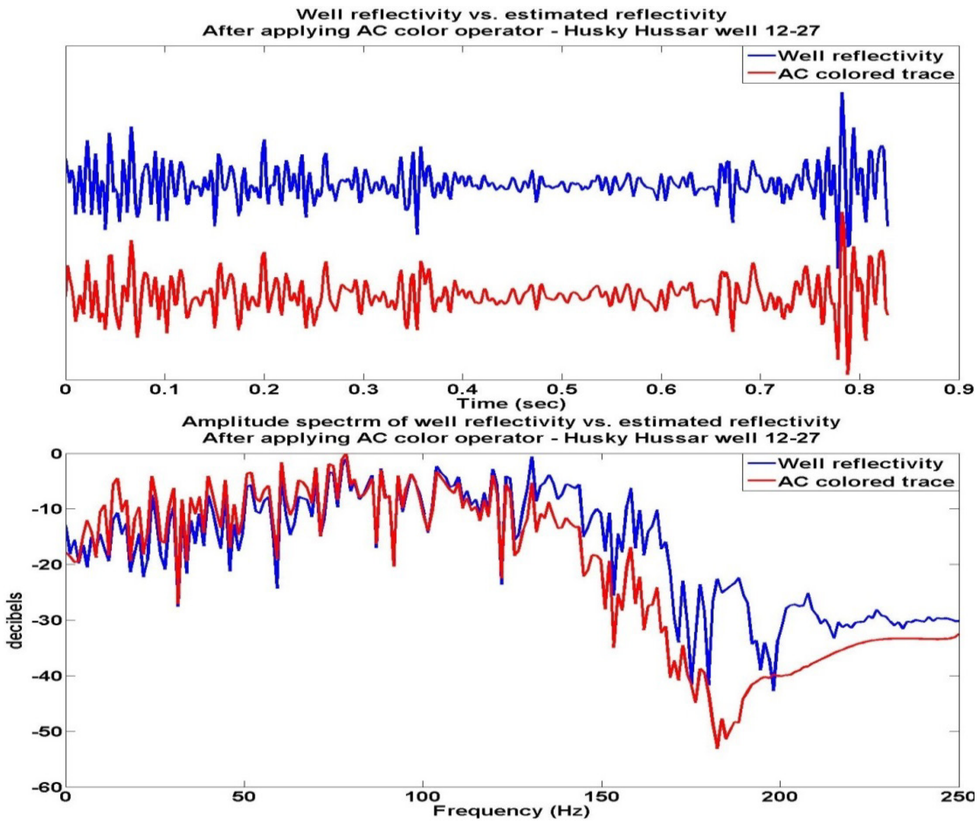

FIG. 7. The result of applying AC color operator to the deconvolved seismic data. The spectral shape of deconvolved data has been improved significantly.

Two other methods to correct the color effects of well reflectivity are minimum phase arctan color operator and sigmoidal color operator (Esmaeili and Margrave, 2014). Like the AC color operator, these color operator also try to model the color trend of reflectivity without reproducing the specific characteristics of reflectivity that must be preserved in the seismic. However, in their method instead of smoothening the reflectivity's amplitude spectrum to create the color operator, they showed this operator can be derived by curve fitting method. Based on the shape of amplitude spectrum of reflectivity, the rolling off shape at the frequencies higher than 130Hz is the result of applying anti-alias filter (Esmaeili and Margrave, 2014). A typical anti-alias filter has an amplitude spectrum which begins to roll off at 50% to 60% of Nyquist frequency and reaches very large attenuation at Nyquist frequency. Thus the shape of this part is artificially rolling off and that means the color operator's amplitude spectrum should be flat for frequencies higher than 130Hz in this case. They suggest two different functions, arctan function and sigmoid function, for fitting to the spectrum of well reflectivity to create the amplitude spectrum of operators and then their phase spectrum are calculating from Hilbert transform of logarithm of their amplitude spectrum. In figure 7 the three different color operators for well 12-27 in time and frequency domain have been shown. This figure shows that two designed color operators, AC color operator and sigmoidal color operator, are closely similar spectral shape at frequencies lower than 50Hz and we are expecting after applying these color operator to the deconvolved data and then computing the acoustic impedance, the prediction can be close.

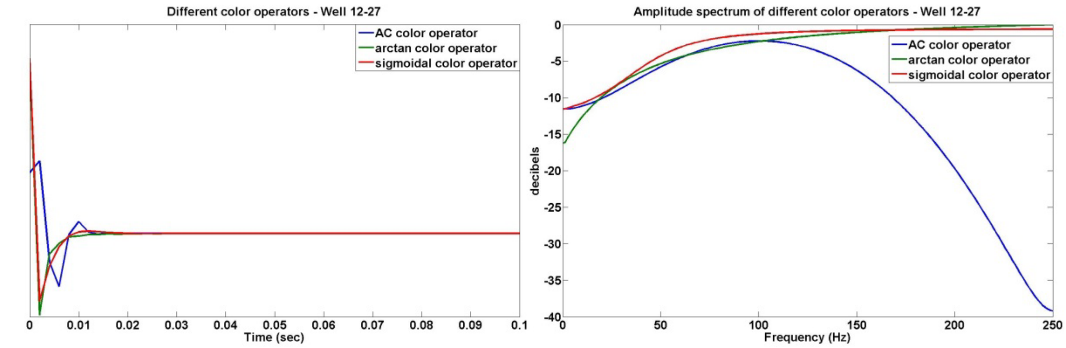

FIG. 8. Different color operators in time and frequency domain.

In the next chapter the effect of different color operators on the real data will be investigated and the calculated acoustic impedance result will be compared with the results of colored inversion.

EFFECT OF COLOR OPERATOR ON REAL SEISMIC DATA

Data preparation

In September 2011, CREWES with cooperation of Husky Energy initiated a seismic experiment near Hussar in Alberta. After the data collected at the filed, the CGG Veritas implemented a specialized processing flow. Normally a high-pass filter is applied to the data to remove noise such as ground roll. This high-pass filter can be as high as 10 Hz. To keep the integrity of the low-frequencies, different noise attenuation was needed. Some of these methods were as follows: removing sinusoidal noise caused by power lines and pump-jacks, attenuating coherent noise and attenuating anomalous high amplitude frequencies. These noise attenuation procedures were repeated several times during the processing flow. Scaling was also specialized as common trace equalization, such as an AGC was undesired. Geometrical spreading gain recovery and surface consistent scaling was implemented instead.

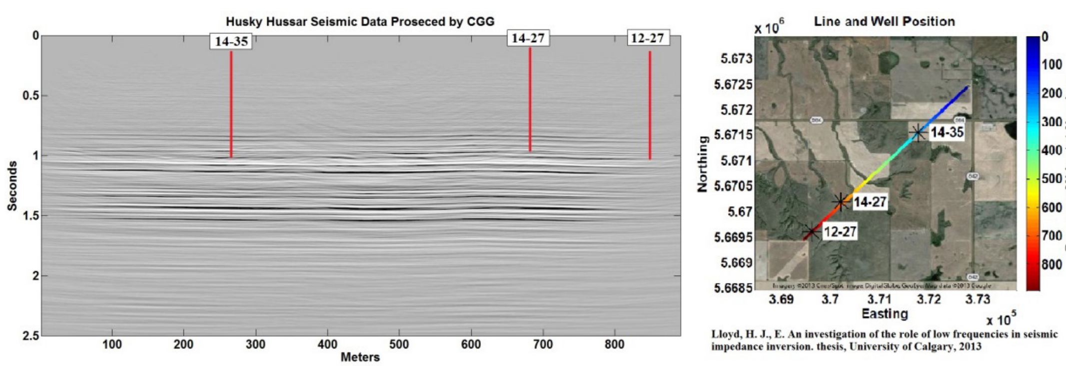

FIG. 9. Husky Hussar seismic data. The data were processed by CGG Veritas.

The fully processed section, Figure 9, when compared to the well reflectivity, has underestimated amplitudes from 0 to 1 second. This may be a result of trying to reduce the noise in the near surface and inadvertently reduced the signal amplitudes as well. This needs to be corrected for but cannot be done with conventional scaling operators such as an AGC as this adversely affects the phase coherence of the data (Isaac et al, 2012) by boosting noise present in the low frequencies that the specialized noise attenuation attempted to reduce. An AGC also equalizes the energy on the trace which does not keep the true relative reflectivity intact. Scaling was achieved by tying well 14-27, using a bulk shift, to the seismic and computing a time variant balancing algorithm with a window size of 50ms and an increment of 10ms. The resulting seismic section from 0 to 1 second is shown in Figure 10. Also, as we know about the geological structure of studied area which is pretty flat, the existing curves on the data at around 1 second are because of the receivers located on top of the hill. Thus, the data need also be flatted. To flatten the data, we chose a target depth as well as the pilot traces. The target depth illustrates which event has a fake curve which needs to be flattened. The appropriate Gaussian window was designed and applied to every traces to focus at the desired event and then the cross correlation of each traces with the pilot traces were calculated. For those of the traces which had the time lag, the time shift applied to the original traces. Figure 11 shows the result of flattened seismic data.

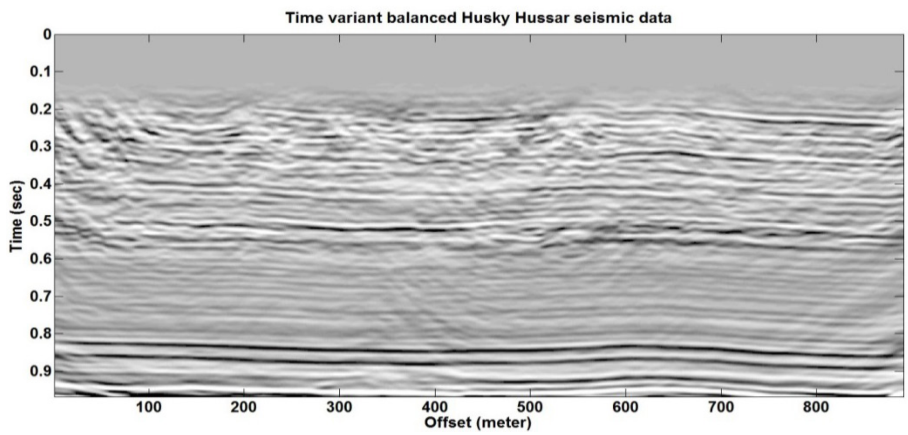

FIG. 10. The seismic data after applying a time variant balancing algorithm with a window size of 50ms and an increment of 10ms.

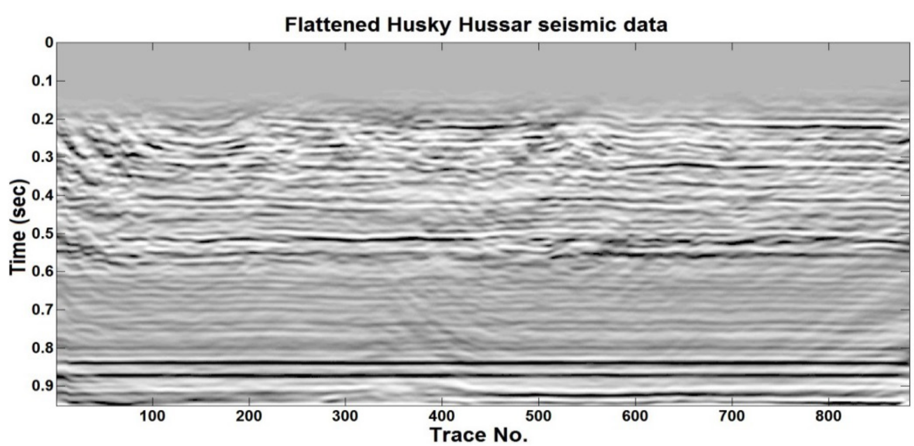

FIG. 11. Based on our knowledge about the geological structure of Hussar, the existed curve on seismic data is not because of structure and they need to be flattened. The flatten algorithm was applied to the seismic data to remove those curves.

Before starting to compute the impedance inversion, the created synthetic data need to be tied with seismic data at the well locations. Related to each well log data, the zero phase synthetic seismic trace was created and compared with the traces in the seismic where the wells are located. Generally, the well tie process includes the time and the phase shift and because of attenuation it may contain an extra time shifts at deeper events. This can be fixed numerically such as dynamic time warping (DTW) method (Cui and Margrave, 2014) or manually by stretching the synthetic trace. Here, after applying 0.002s, 0.044s and -0.014s time shift for synthetic seismic traces of wells 14-35, 14-27 and 12-27 respectively, the time stretching also needs to be applied to the synthetic data. Figures 12 and 13 are showing three synthetic traces and their belonged seismic traces after applying the mentioned time shifts and time stretching respectively.

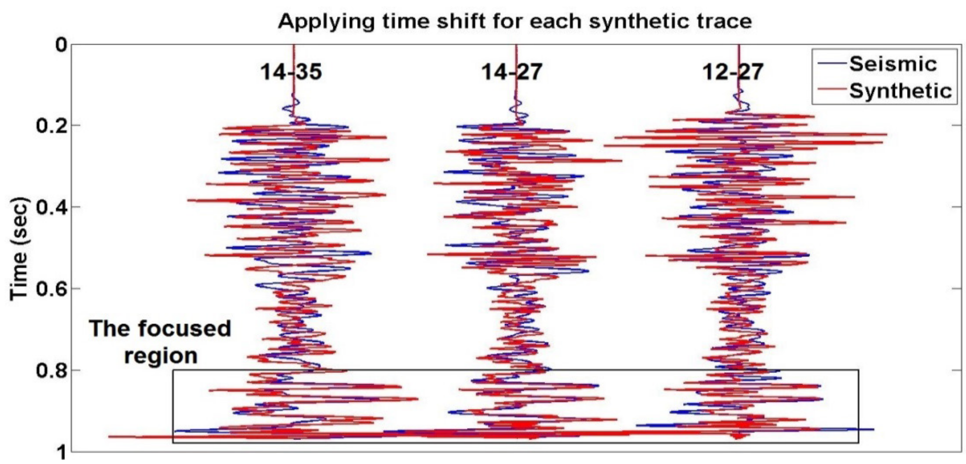

FIG. 12. For time shifting the created synthetic data to tie to the seismic trace, the region was defined to be focused to calculate the appropriate time shifting which each synthetic trace needs to be done.

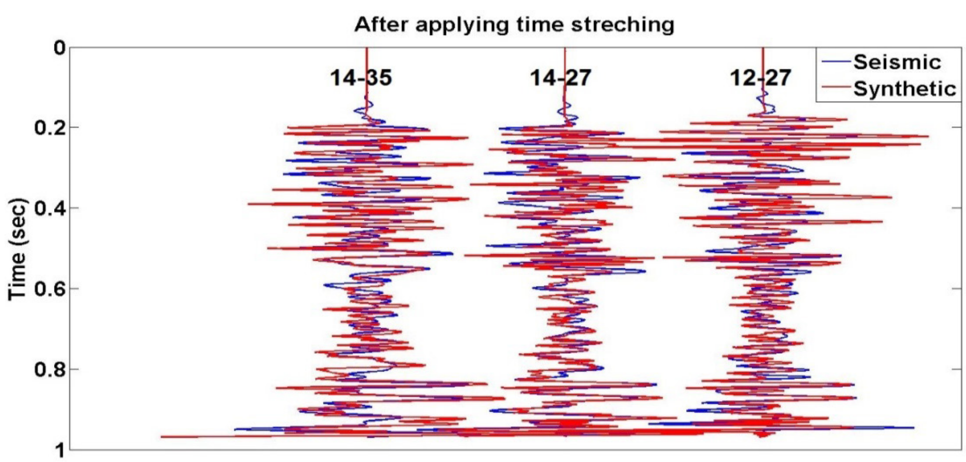

FIG. 13. After applying appropriate time shifting (and if applicable phase shifting), because of attenuation, different time slices might need different time shifts. This can be done by time stretching algorithm.

As can be seen from the second figure, at all three well locations there are good matches between seismic traces and synthetic traces. The calculated cross correlations between each synthetic and seismic pairs are 0.5561, 0.5370 and 0.5588 for wells 14-35, 14-27 and 12-27 respectively and all of them have been occurred at zero lag.

Color operator effects on seismic data and impedance inversion

Once the synthetic seismic data successfully tied to the seismic data, we can apply different color operators to the seismic section. With two different methods we can apply the color operators. We can average the three color operators which created from three Hussar wells and then applying it into the entire seismic section or, we can use the spatial interpolation of three color operators and then applying it to the seismic section. Here, all the color operators for whole the studied area have been created with the spatial interpolation of three wells. Once it has been done, each trace of seismic section can be convolved with its related color operator. The result of applying minimum phase arctan and sigmoidal color operators to the seismic section are shown in the figures 14 and 15. At each figure the right hand side one is before applying color operator and the left hand side is after applying color operator.

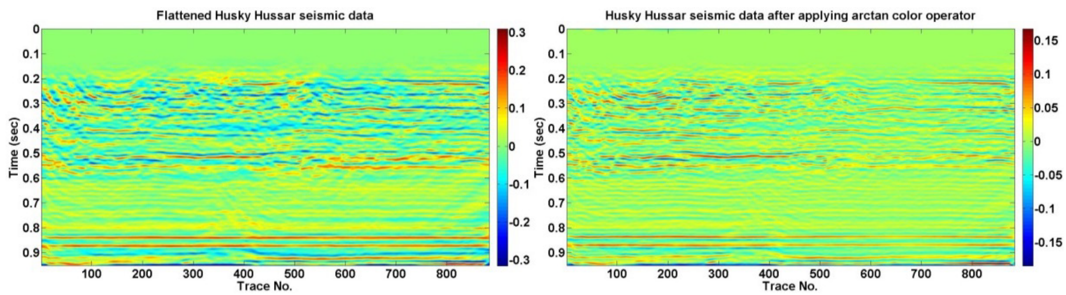

FIG. 14. The effect of arctan color operator on Hussar seismic data.

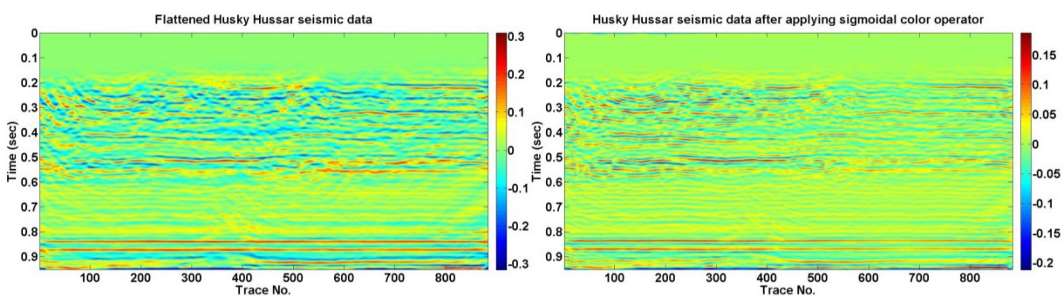

FIG. 15. The effect of sigmoidal color operator on Hussar seismic data.

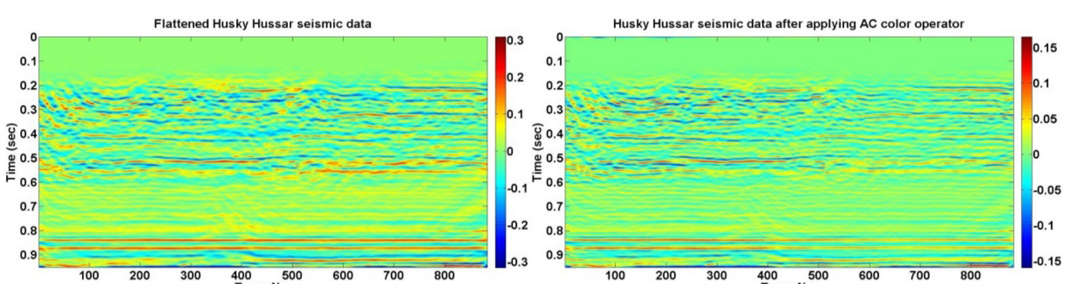

FIG. 16. The effect of AC color operator on Hussar seismic data.

	Well 14-25	Well 14-27	Well 12-27
Before color op.	0.5561	0.5370	0.5588
After arctan	0.6083	0.6193	0.6300
After sigmoidal	0.5917	0.5845	0.6129
After AC	0.6095	0.5851	0.6067

Table 1. The calculated maximum correlation between estimated data and well reflectivity data at the location of each well before and after applying color operators.

Table 1 shows the maximum correlation between the well reflectivity and the seismic traces located at each well location. The results have been calculated for seismic sections before and after applying color operators and they show the color operators can increase the reflectivity's correlation. Comparing the amplitude spectrum in frequency domain, for example for seismic trace at the well 14-27 location, showing the improvement at seismic's amplitude spectrum after applying color operator.

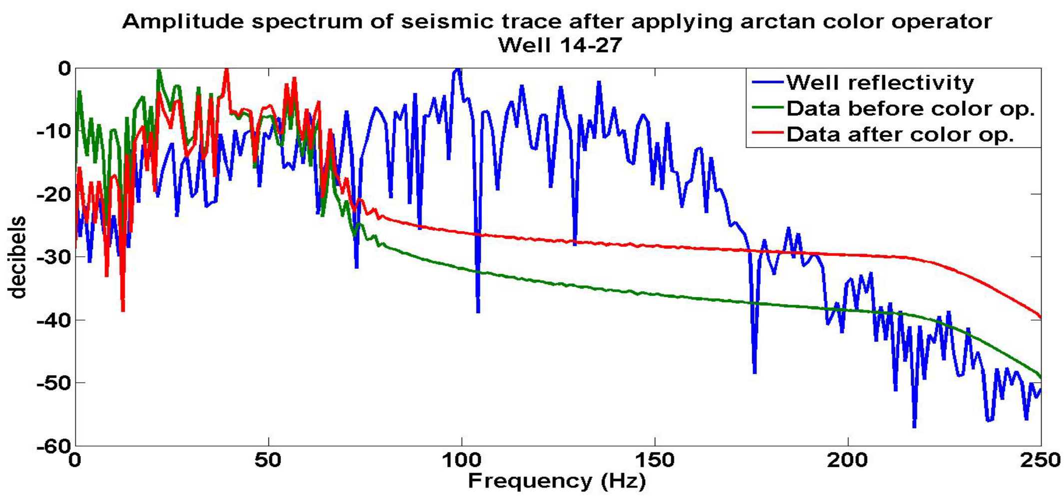

FIG. 17. An example of applying sigmoidal color operator on Hussar seismic data. The trace has been picked near the well 14-27.

Figure 18 shows the impedance inversion result from using the recursion formula for before and after applying arctan color operator to the seismic section. This figure shows that applying color operator to the seismic section can effectively recover part of impedance section which related to the major events located at around t=8.5s. However, from figure 17, because the majority of frequencies higher than 70Hz are not available in the estimated reflectivity section, thus the impedance estimation section is out of any detailed events.

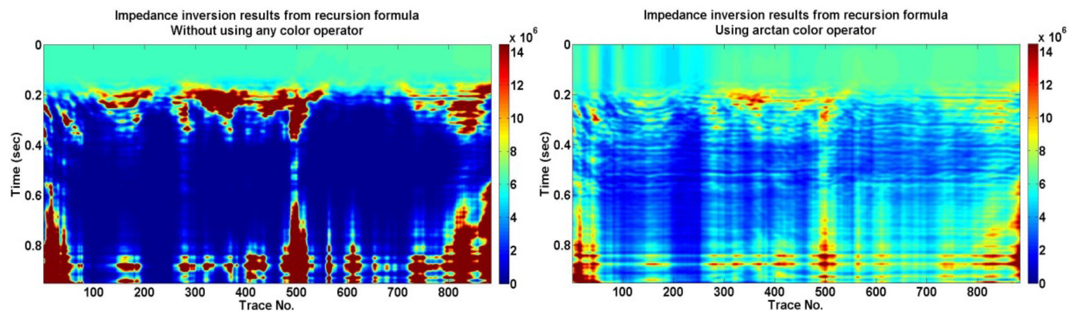

FIG. 18. Impedance inversion using recursion formula for the seismic data before and after applying color operator.

As mentioned before, the BLIMP inversion algorithm extracts the low and high frequency data from well log data. Based on figure 17, even after applying color operator to the seismic data the frequencies lower than 5Hz are missing and BLIMP can put these data from well log data. To find the value of high frequencies needed to be applied from well logs; again it is possible to look at the amplitude spectrum of seismic traces from the beginning point of the seismic line to its end point. The observation suggests that the high frequency value for the BLIMP algorithm can be linearly varied from 50Hz at the well 12-27 side to the 60Hz at the well 14-35 side. The results of impedance inversion computed with BLIMP algorithm are shown in the next four figures. The well impedance traces are separated at their location. These results clearly demonstrate that after applying any color operator (especially the arctan color operator) to the seismic data the impedance estimation can be improved significantly.

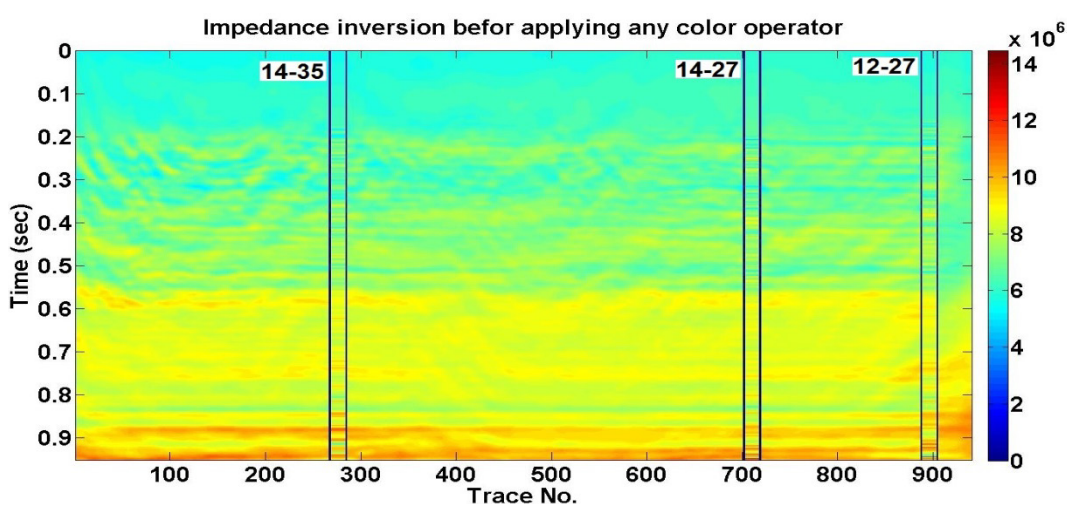

FIG. 19. The BLIMP impedance inversion without using any color operator. The low frequency in BLIMP algorithm was chosen 5Hz and the high frequency is linearly varying from 60Hz to 50Hz from left to the right side of seismic section.

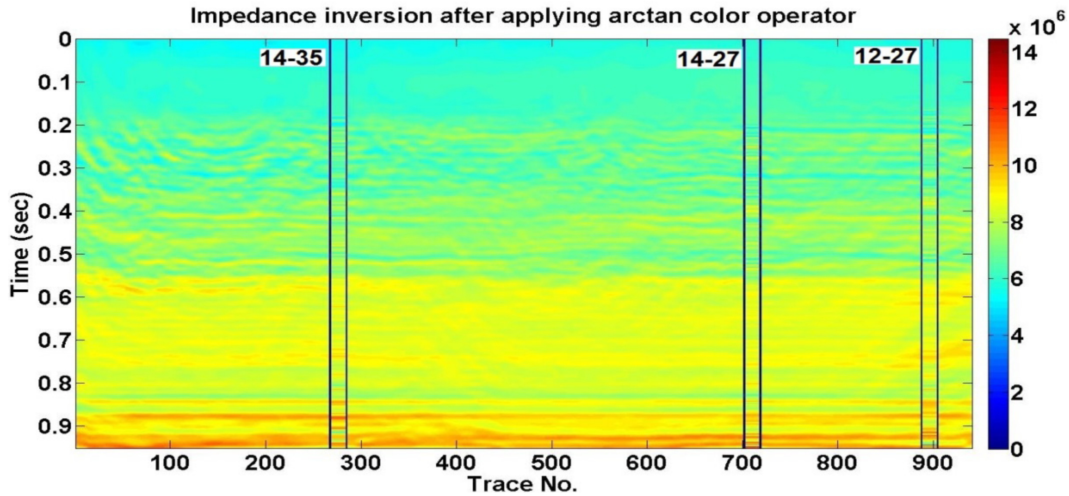

FIG.20. The BLIMP impedance inversion for arctan color operator. The low frequency in BLIMP algorithm was chosen 5Hz and the high frequency is linearly varying from 60Hz to 50Hz from left to the right side of seismic section.

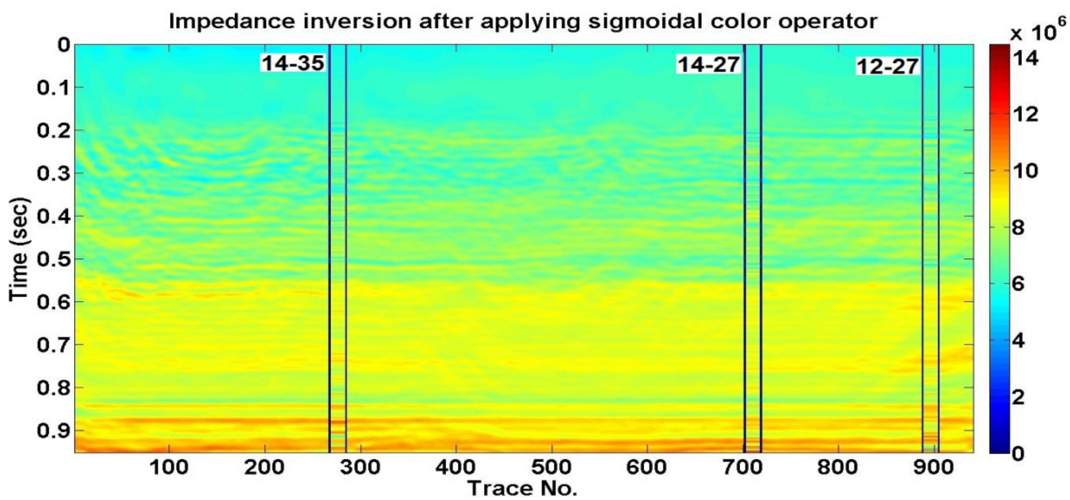

FIG.21. The BLIMP impedance inversion for sigmoidal color operator. The low frequency in BLIMP algorithm was chosen 5Hz and the high frequency is linearly varying from 60Hz to 50Hz from left to the right side of seismic section.

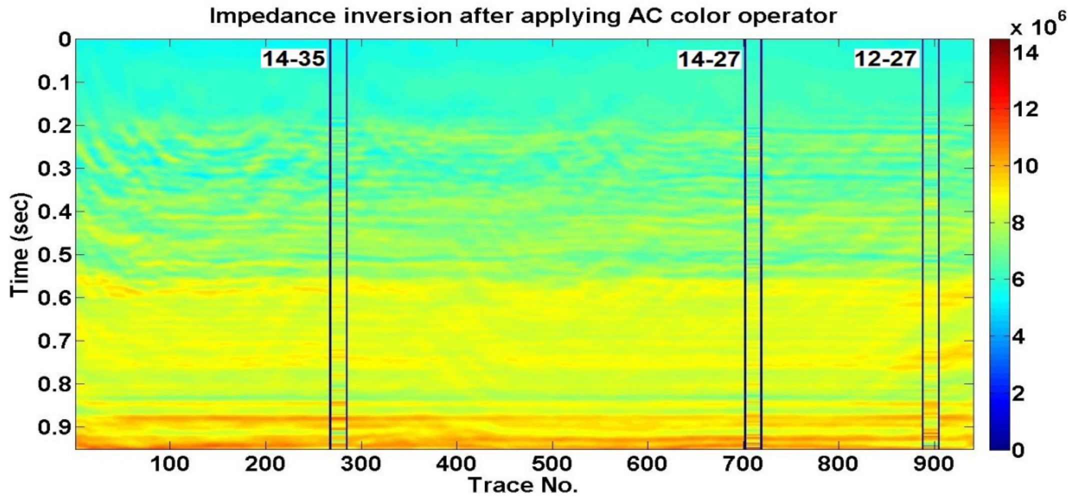

FIG. 22. The BLIMP impedance inversion for AC color operator. The low frequency in BLIMP algorithm was chosen 5Hz and the high frequency is linearly varying from 60Hz to 50Hz from left to the right side of seismic section.

The colored inversion also can be applied to the seismic traces and the appropriate scale factor to get the impedance result can be found from detrended average well impedance. The averaging is done to remove local effects. Its result can be seen in the figure 23.

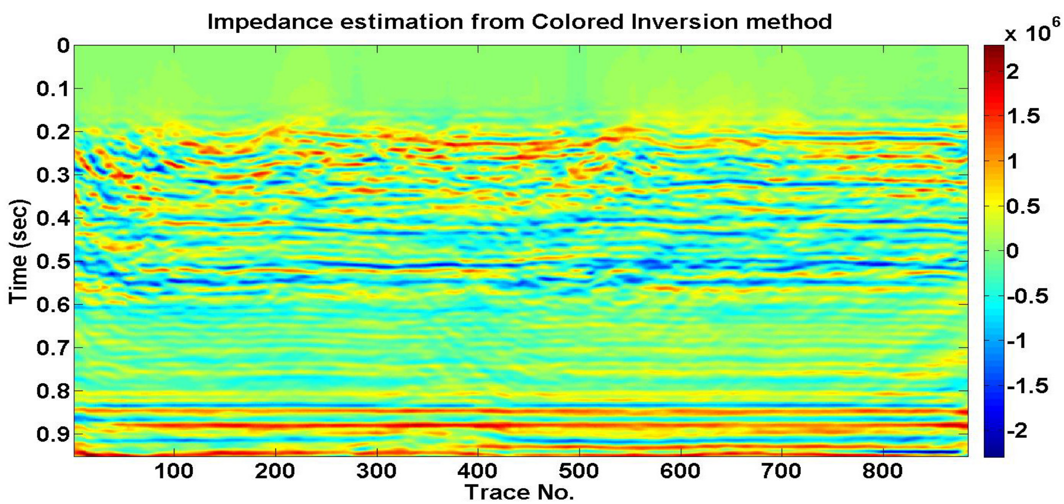

FIG. 23. The impedance estimation from colored inversion method. This method does not have any low frequencies and the estimated values are just the estimation of impedance variation around its trend.

As we can see, the colored inversion method can estimate the acoustic impedance very detailed. However, the most important point about this method is the value of impedance. As can be seen from figure 23, the calculated impedance has both positive and negative values. But, as we know from impedance definition (velocity multiply density), this value cannot be a negative value. The computed impedance in this case is only showing the variation of impedance from its trend not its real value. On the other hand, as we can see in the figure 24, the broadband impedance inversion can be divided into the two separate parts: the low frequency part which is belonged to the trend of broadband impedance and the high frequency part which belonged to the impedance fluctuation.

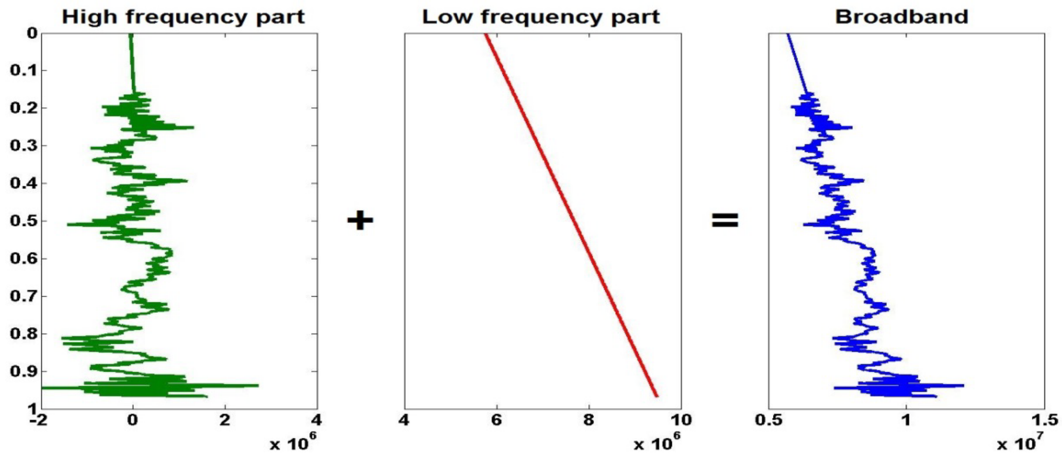

FIG. 24. The schematic of how the broadband acoustic impedance can be separated into the two part. Low frequency part and high frequency part.

Thus, the colored inversion method is a robust and fast way to estimate the impedance variation without any low frequency components. The other investigation about this method, as previously mentioned, the colored inversion method is approximately equivalent with the -90 degree phase rotation which means, if -90 degree phase rotation has been applied to the seismic data and then it balances with the detrended average well impedance; we can get closely the same results as colored inversion (figure 25)

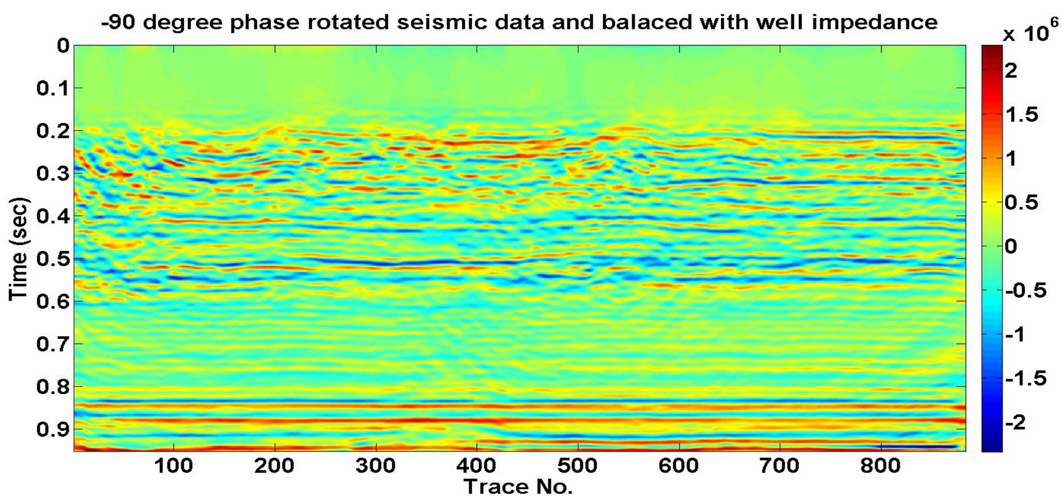

FIG. 25. The -90 degree phase rotation was applied to the seismic section and then has been balanced with the detrended average well impedance. The results are suggesting both -90 degree phase rotation and colored inversion can be equivalent.

To get the true impedance estimation it can be possible to add the trend of average well impedance to the impedance result of either colored inversion or -90 degree phase rotated seismic data.

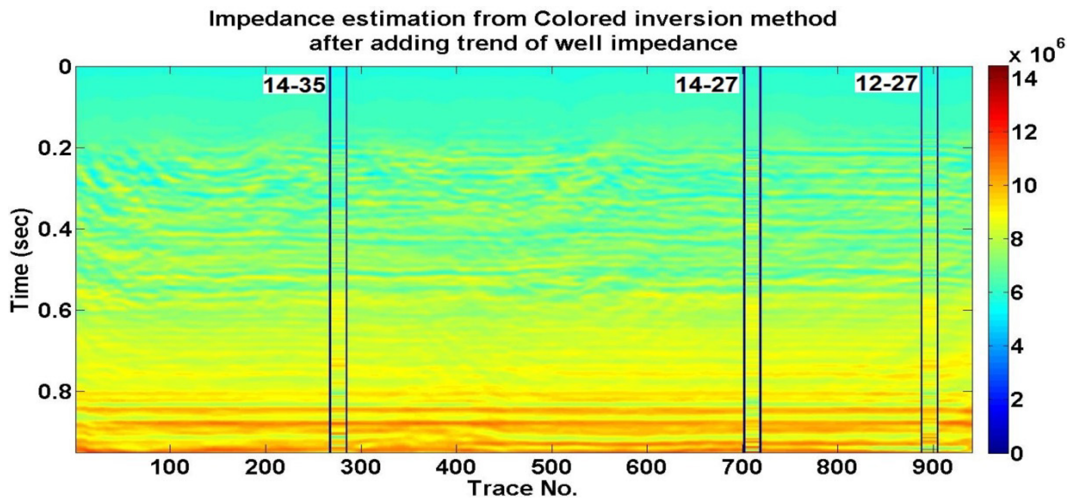

FIG. 26. The trend of average well impedance is added to the colored inversion to obtain the true impedance inversion.

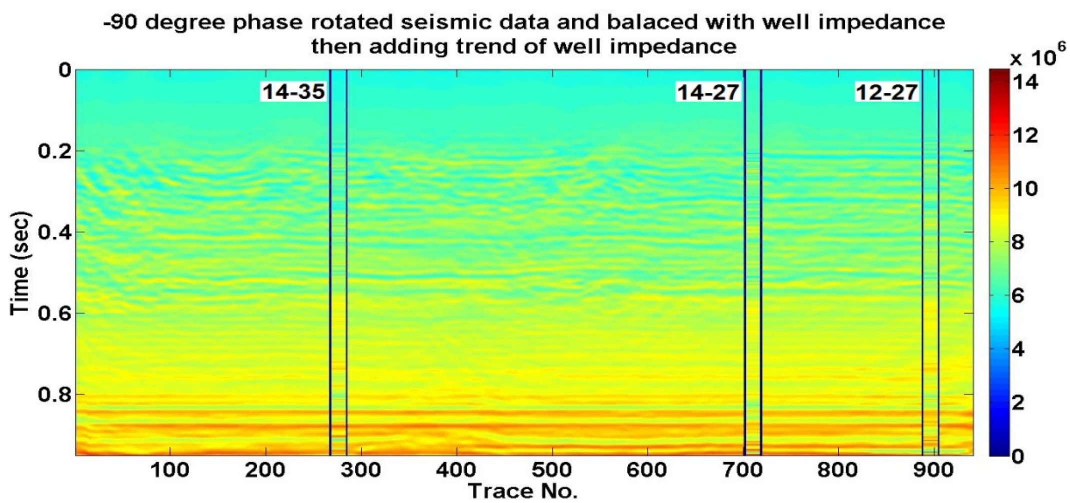

FIG. 27. The trend of average well impedance is added to the -90 degree seismic section to obtain the true impedance inversion.

The last step is comparing the different methods in impedance inversion results. As it has been seen, the colored inversion method was completely different than the other methods we introduced here. The colored inversion method was estimating the acoustic impedance with mostly high frequency components and without any low frequencies which makes its mean value is becoming so small (10^3) in comparing with impedance value which is around 10^7. Thus, we will compare three different impedance resulted from color operators in low frequency components with the well impedance and then in high frequency component after applying 10Hz high pass filter to their impedance results as well as well impedance, they can be compared with colored inversion and -90 degree phase rotation impedance result.

For comparing the low frequency components, the maximum correlation has been calculated for each impedance result and they are shown in the table 2. Note that because of the mentioned reason, the results only include using color operators. For better illustration, their maximum correlations also have been presented in the charts 1. From the chart, generally we can say after using any of the color operators, the maximum correlation between the inverted impedance and well impedance can be improved.

	Well 14-35	Well 14-27	Well 12-27
Without any color op.	0.8556	0.8439	0.8123
arctan color op.	0.9939	0.9928	0.9931
sigmoidal color op.	0.9925	0.9920	0.9928
AC color op.	0.9924	0.9920	0.9928

Table 2. The maximum correlation calculated for between estimated impedance and Hussar well impedance at the well locations.

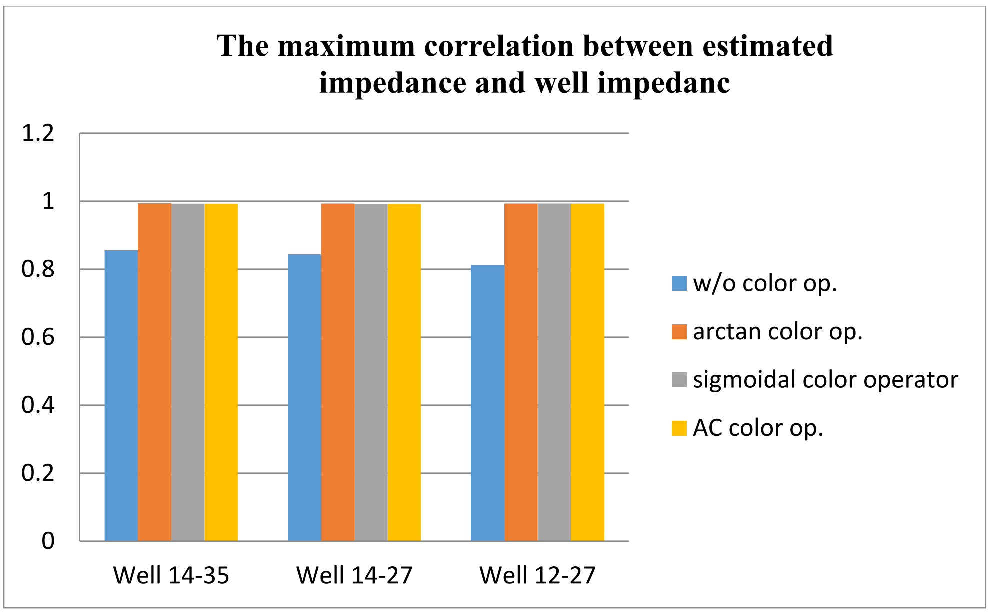

Chart 1. The chart based on the maximum correlation values presented in table 2 which are between estimated impedance and Hussar well impedance at the well locations.

And finally, for comparing the high frequency components the 10Hz high pass filter was applied to all the estimated inversion and well impedance except the colored inversion and -90 degree phase rotated seismic data. The result of maximum correlation between estimated impedance and well impedance are illustrated in table 3 and chart 2.

	Well 14-35	Well 14-27	Well 12-27
Without any color op.	0.2915	0.2261	0.2169
arctan color op.	0.3568	0.4024	0.3460
sigmoidal color op.	0.3726	0.4488	0.3664
AC color op.	0.3726	0.4483	0.3632
Colored inversion	0.2602	0.2472	0.2392
-90 degree phase rotation	0.2257	0.2731	0.2441

Table 3. The maximum correlation values between estimated impedance and Hussar well impedance. The 10Hz high pass filter was applied to all the estimated inversion and well impedance except the colored inversion and -90 degree phase rotated seismic data.

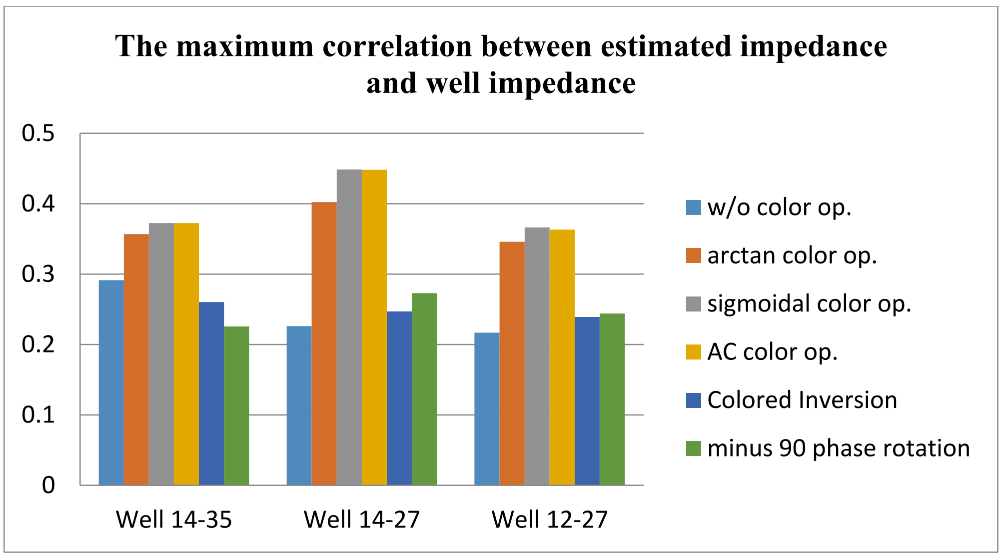

Chart 2. The chart based on the maximum correlation values presented in table 3 which are between estimated impedance and Hussar well impedance at the well locations.

CONCLUSION

To estimate the acoustic impedance more precisely the well log information is always mandatory and as we showed for deriving and applying the color operators or doing the colored inversion, both methods need the frequency information from the log. However, our observation demonstrates using the color operators to correct the color properties of data, and beside of that using the BLIMP algorithm, the impedance estimation can be improved significantly. Also, in this study it has been showed that the impedance section can be easily calculate by only applying -90 degree phase rotation to the seismic data and this is because of applying the integral operator on seismic data in the impedance calculation (recursion formula) where this operator mathematically causing -90 degree phase rotation.

ACKNOWLEDGEMENTS

The authors thank the sponsors of CREWES for continued support. This work was funded by CREWES industrial sponsors and NSERC (Natural Science and Engineering Research Council of Canada) through the grant CRDPJ 461179-13. And also we would like to thank all the students and staff in CREWES.

REFERENCES

Cui, T., & Margrave, G. F. (2014). *Drift time estimation by dynamic time warping.* CREWES Research Report, Vol 26.

Esmaeili, S., & Margrave, G. F. (2014). *Improving frequency domain deconvolution at low frequencies.* CREWES Research Report, Vol. 26.

Esmaeili, S., & Margrave, G. F. (2014). *The optimum color operator for recovering low frequencies.* CREWES Research Report, Vol. 26.

Ferguson, R. J., & Margrave, G. F. (1996). A simple algorithm for bandlimited impedance inversion. *CREWES research report, Vol. 8, No. 21.*

Galbraith, J. M., & Millington, G. F. (1979). Low frequency recovery in the Inversion of seismoerams. *Journal of the CSEG, v. 15*, p. 30-39.

Hunt, L., Gray, F. D., & Wallace, R. A. (1993). Using Reflectivity to Produce a Superior Deconvolution. *Canadian SEG Convention Technical Abstracts*, 95-96.

Isaac, J. H., Margrave, G. F., Deviat., M., & Nagarajappa, P. (2012). *Processing and analysis of Hussar data for low frequency content.* CREWES Research Report, Vol. 24.

Lancaster, S., & Whitcombe, D. (2000). Fast-track 'colored' inversion. *SEG Technical Program Expanded Abstracts 2000*.

Lavergne, M., Willm, C., & . (1977). Inversion of seismograms and pseudovelocity logs. *Geophys. Proso, v. 25*, p. 231 - 250.

Lindseth, R. O. (1979). Synthetic sonic logs-a process for stratigraphic interpretation. *Geophysics*, 3-26.

Oldenburg, D. W., Scheuer, T., & Levy, S. (1983). Recovery of the acoustic impedance from reflection seismograms. *Geophysics*, 1318-1337.